

Chapter 29

An Experimental Study on Characteristics of Rolling in Head Waves for a Vessel with Nonlinear GZ-curve



Toru Katayama, Shugo Miyamoto, Hirotada Hashimoto and Yoshifumi Tai

Abstract In this study, the characteristics of rolling in head waves for a vessel with strong nonlinear GZ -curve, which includes parametric rolling, are investigated. Rolling is measured for systematically changed wave length and height under the same forward speed, which is service speed in heavy weather. As a result, the range of T_e/T_ϕ (T_e and T_ϕ are encounter wave period and the roll natural period of the model) when oscillatory rolling occurs is wider than that of previous results by Taguchi et al. (Model Experiment on Parametric Rolling of a Post-Panamax Containership in Head Waves. Proceedings of the Ninth International Conference on Stability of Ships and Ocean Vehicles, 2006), and the range spreads out wide area of $T_e/T_\phi > 0.5$. Especially, in the range of $T_e/T_\phi > 0.5$, oscillatory rolling is caused by large wave height and roll amplitude becomes larger than that at $T_e/T = 0.5$. It is supposed that the result is caused by change of roll natural period caused by nonlinear GZ -curve. In order to confirm it, numerical simulations are carried out for several variations of GZ -curve. Additionally, roll measurements in irregular waves with Pierson-Moskowitz spectrum are also carried out.

Keywords Parametric rolling · Wide-breadth and shallow-draft
Strongly nonlinear- GZ -curve

T. Katayama (✉) · S. Miyamoto
Graduate School of Engineering, Osaka Prefecture University, Sakai, Japan
e-mail: katayama@marine.osakafu-u.ac.jp

S. Miyamoto
e-mail: ss103029@edu.osakafu-u.ac.jp

H. Hashimoto
Graduate School of Engineering, Osaka University, Sakai, Japan
e-mail: hashimoto@port.kobe-u.ac.jp

Y. Tai
Imabari Shipbuilding Co., Ltd, Imabari, Japan
e-mail: tai.yoshifumi@imazo.com

29.1 Introduction

Ballast water for vessels is significant to prevent their stability and propulsion performance losses, which are caused by their light-draught. However, the International Maritime Organization (IMO) adopted International Convention for the Control and Management of Ships' Ballast Water and Sediments in 2004, because of avoiding its environmental impact.

Then, in order to solve this problem, new hull forms are being designed, which use a small amount of ballast water or don't need ballast water. For example, one of new designed hull has shallow draft and wide breadth. Such hull may show different roll characteristics from the conventional vessels.

In the previous study (Tai et al. 2011), for a shallow draft and wide breadth vessel, its roll characteristics in beam waves have been investigated experimentally. The results show that its roll natural period is changed by its roll amplitude and its roll resonance occurs in different wave period depending on different wave height.

In this study, the roll characteristics of the same model (Tai et al. 2011) in head waves (including parametric rolling) are investigated. Roll measurements in regular head waves are carried out. From the results, it is found that large amplitude rolling occurs at a wider range of encounter frequencies than that of a conventional vessel, and it is supposed that it is caused by strong nonlinearity of its GZ -curves. Then, in order to be clear the reasons of the results, numerical simulations are carried out. Additionally, the roll characteristics in irregular waves with Pierson-Moskowitz spectrum are also investigated.

29.2 Model and Measurement

Figure 29.1 and Table 29.1 show a body plan and principal particulars of a model. Figure 29.2 shows the calculated GZ -curve of the model in real scale. In the same figure, the linear GZ -value of the model is also shown. The calculated GZ -curve shows strong nonlinear characteristics in the range of small roll angles. This is because bilge of the model is exposed above the water surface from the range of small roll angles.

Figure 29.3 shows measured roll natural period of the model by a free decay test, which is carried out for various initial heel angles. This figure shows that the roll natural period becomes longer according to increase in roll amplitude. And this is caused by the strong nonlinearity of the GZ -curve shown in Fig. 29.2.

In order to investigate the occurrence of oscillatory rolling, towing tests in regular head waves are carried out at the towing tank of Osaka Prefecture University (length 70 m, breadth 3 m, depth 1.5 m). Figure 29.4 shows a schematic view of the experiment. A model is attached to the towing carriage with two elastic ropes (Hashimoto et al. 2007). The model is towed at constant forward speed in head waves, and a small disturbance which is heel caused by hand is given. Roll motion is measured

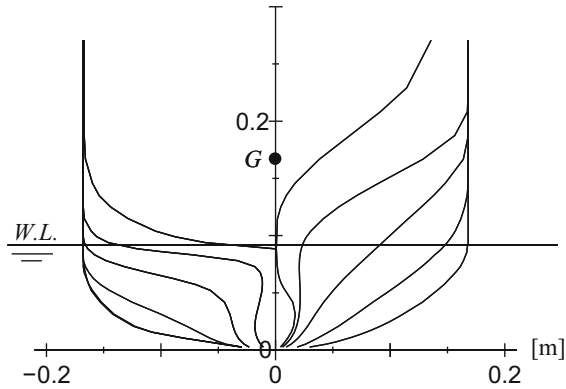
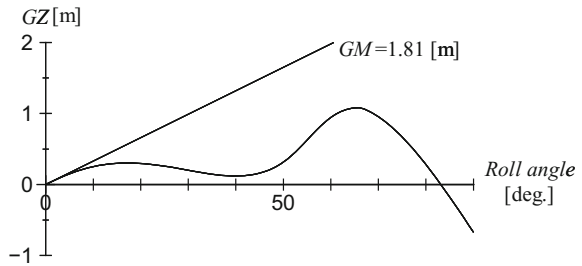


Fig. 29.1 Body plan of the model

Table 29.1 Principal particulars of the model

	Ship	Model
L_{pp} [m]	192	2.0
B [m]	32.26	0.336
draft: d [m]	9.0	0.0938
KG [m]	17.0	0.177
GM [m]	1.81	0.0189
Roll natural period: T_ϕ [sec]	18.42	1.88
Breadth of bilge-keels	0.7	0.0073
Position of bilge-keels	s.s. 3.34–s.s. 5.59	

Fig. 29.2 Calculated GZ -curve of the model in real scale



by a gyroscope (CROSSBOW NAV440) and wave elevation is also measured by a servo type wave height meter attached to the towing carriage.

Fig. 29.3 Measured roll natural period of the model

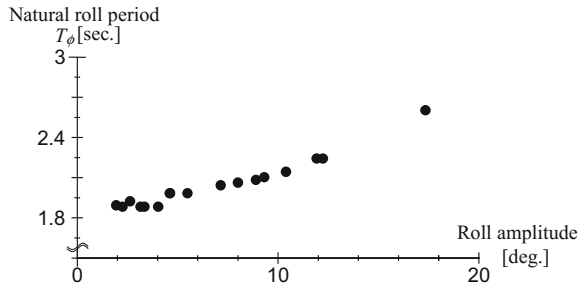
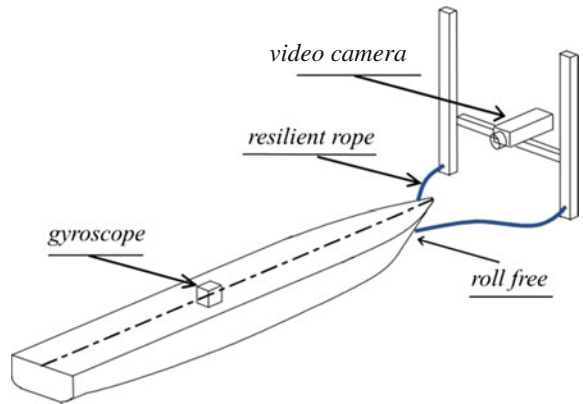


Fig. 29.4 Schematic view of the experiment



29.3 Roll Measurement in Regular Head Waves

Table 29.2 shows the experimental conditions. When the model is towed at $F_n = 0.083$ in head wave of $T_w = 1.05$ s, the encounter wave period is half of the roll natural period ($T_\phi = 1.88$ s) for small amplitude. This F_n is 7 kts in the real scale.

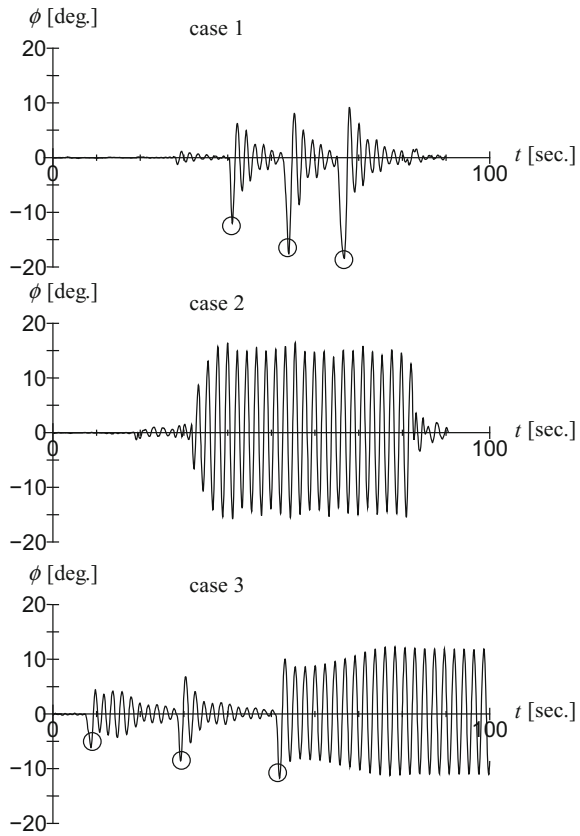
Figure 29.5 shows examples of typical time histories of measured rolling in regular head waves. The upper figure shows the result that oscillatory rolling does not occur. The middle figure shows the result that oscillatory rolling occurs. The bottom figure shows the result that oscillatory rolling occurs after a small disturbance which is

Table 29.2 Experimental condition

F_n	0.083
Wave period: T_w [sec]	0.99–1.55
T_e/T_ϕ	0.42–0.71
Wave height: H_w [m]	0.01–0.05

T_e : encounter wave period, T_ϕ : roll natural period

Fig. 29.5 Time histories of measured roll motions in regular head waves. (O:disturbance)



heel caused by hand, this phenomenon is investigated as a bi-stability mechanism by Spyrou et al. (2008).

Figure 29.6 shows measured roll amplitudes in regular head waves. In this figure, its horizontal axis is the ratio of encounter wave period to the roll natural period for small amplitude. At $T_e/T_\phi = 0.5$, oscillatory rolling occurs for any wave heights. For small wave height $H_w = 0.01$ m, oscillatory rolling does not occur except at $T_e/T_\phi = 0.5$.

Figure 29.7 shows the measured roll amplitude of a conventional post-panamax container vessel by Taguchi et al. (2006) in order to compare with Fig. 29.6. From the comparisons, it is noted that the range of T_e/T_ϕ where oscillatory rolling occurs in Fig. 29.6 is wider than that of Fig. 29.7 even if its amplitude is smaller, and the range of Fig. 29.6 spreads wider area of $T_e/T_\phi > 0.6$. Especially, at the range over $T_e/T_\phi = 0.5$. in Fig. 29.6, oscillatory rolling is caused by large wave height, and its amplitude becomes larger than that at $T_e/T_\phi = 0.5$. It is supposed that the spread of occurrence of large amplitude rolling to wider area of $T_e/T_\phi > 0.5$ in Fig. 29.6 is caused by the strong nonlinearity of GZ -curves.

Fig. 29.6 Measured roll amplitude in regular head waves at $F_n = 0.083$, (Case 3: $T_e/T_\phi = 0.53, 0.55, 0.58$ at $H_w = 0.02$ m, $T_e/T_\phi = 0.61$ at $H_w = 0.03$ m, $T_e/T_\phi = 0.63$ at $H_w = 0.04$ m)

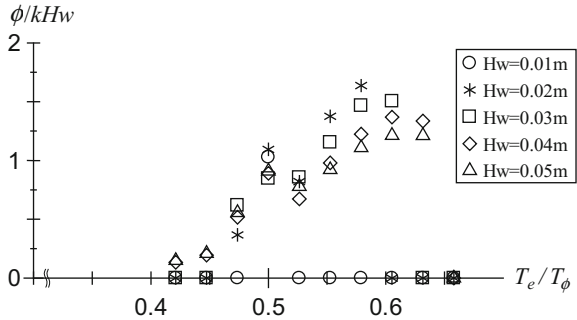


Fig. 29.7 Measured roll amplitude in regular head waves at $H_w = 0.11$ m. (citation from Fig. 6 in Taguchi et al. 2006)

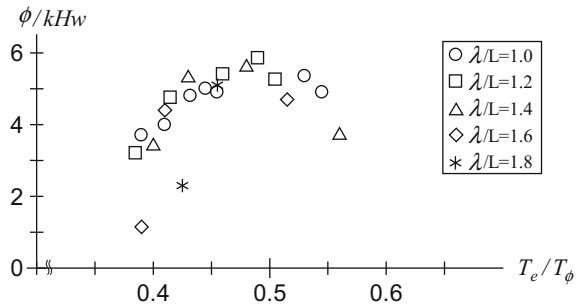


Table 29.3 Experimental conditions

λ/L_{pp}	1.0		
F_n	0.000	0.032	0.077
T_e/T_ϕ	0.60	0.55	0.5

Table 29.3 shows the experimental condition for the roll measurement in regular head waves with constant wave length ($\lambda/L_{pp} = 1$). When model is towed at $F_n = 0.077$, its encounter wave period is half of the roll natural period for small amplitude ($T_\phi = 1.88$ s). According to decrease in forward speed, its encounter period becomes long.

Figure 29.8 shows the measured roll amplitude. In this figure, roll amplitude increases according to decrease in forward speed, even if T_e/T_ϕ becomes larger than 0.5.

In order to make its reason clear, the characteristics of roll damping is investigated by using Ikeda’s method, and roll amplitude is estimated by using a simplified estimation for amplitude of parametric rolling (Katayama et al. 2009) .

Figure 29.9 shows the estimated roll damping. The roll damping decreases according to decrease in forward speed. It is caused by decrease in the lift component of roll damping which is caused by forward speed.

Figure 29.10 shows the estimated roll amplitude by Eq. (29.1) (Katayama et al. 2009).

Fig. 29.8 Measured roll amplitude

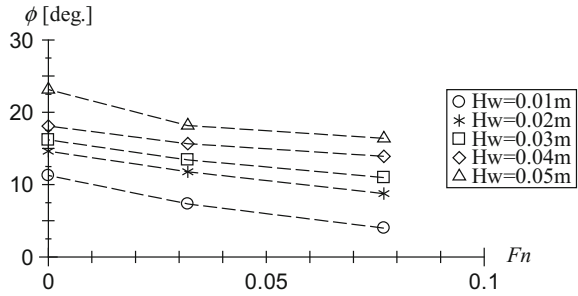


Fig. 29.9 Estimated roll damping coefficient by Ikeda's method

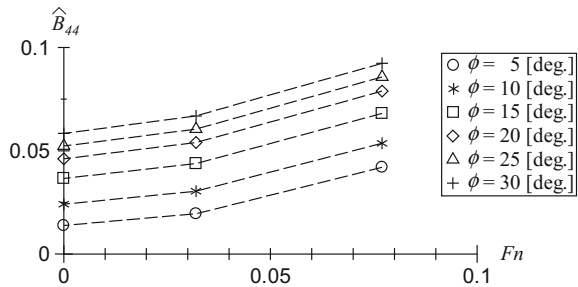
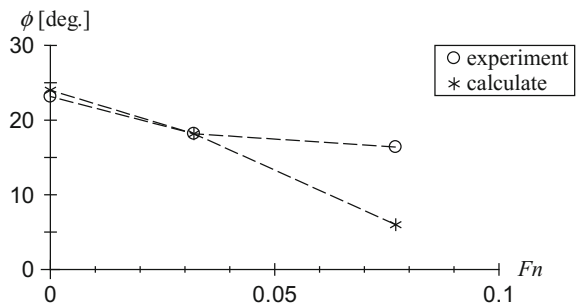


Fig. 29.10 Estimated roll amplitude by Eq. (29.1). ($H_w = 0.05$ m)



$$B_{44}(\phi_a) = \frac{W \Delta GM}{2\omega_e} \tag{29.1}$$

The measured results are also shown in the same figure. Both results show the same tendency for change of forward speed.

From these results, it is understood that decrease in forward speed causes decrease in roll damping, and roll amplitude becomes larger. On the other hand, roll natural period becomes long according to increase in roll amplitude as shown in Fig. 29.3. Then rolling resonates with increased wave encounter period by decrease in forward speed, and parametric rolling occurs.

29.4 Roll Measuring in Irregular Head Waves

Equation (29.2) is one of Pierson-Moskowitz spectrum.

$$S(\omega) = \frac{8.1 \times 10^{-3} \times g^2}{\omega^2} \exp\left(-\frac{3.11/H_{1/3}^2}{\omega^4}\right) \tag{29.2}$$

To make irregular waves, the spectrum is divided into 1000 equally in $\omega = 1\text{--}15$ rad/sec and a sine wave of each frequency component is superposed. In addition, the phase difference of each frequency component is given as random numbers. The number of measurements is decided by the convergence of variance of rolling (Appendix).

In this study, roll measurements are carried out for three significant wave heights, and Fig. 29.11 shows the power spectral densities obtained from the measured wave elevations.

Figure 29.12 shows the probability distributions of the measured roll amplitudes. In this measurement, roll amplitude is not over 10 deg at significant wave height = 0.04 m. The results show that the roll amplitude increases with increase in significant wave height.

Fig. 29.11 Measured power spectral density of wave height. (1/3 significant wave height = 0.04, 0.05, 0.06 m)

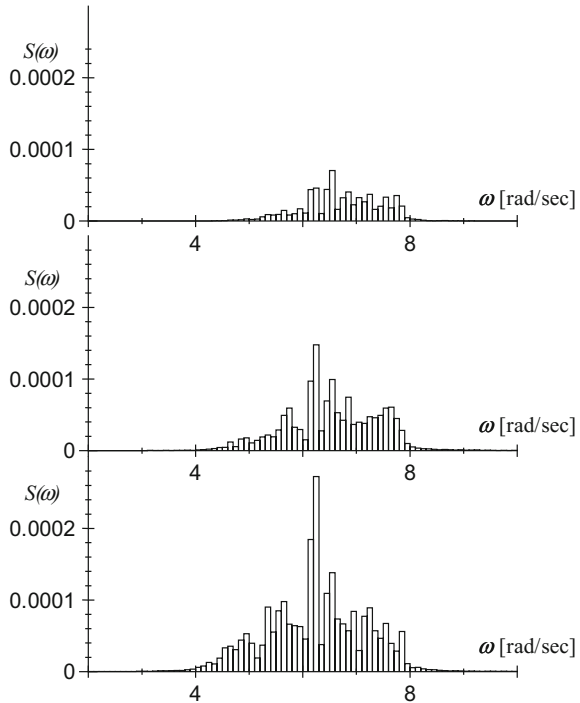


Fig. 29.12 Probability distribution of roll amplitude. (significant wave height = 0.05, 0.06 m)

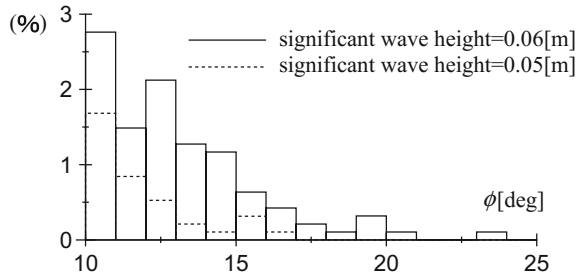


Fig. 29.13 Time histories of measured wave height and roll motion in irregular head waves at $H_w = 0.06$ m.)

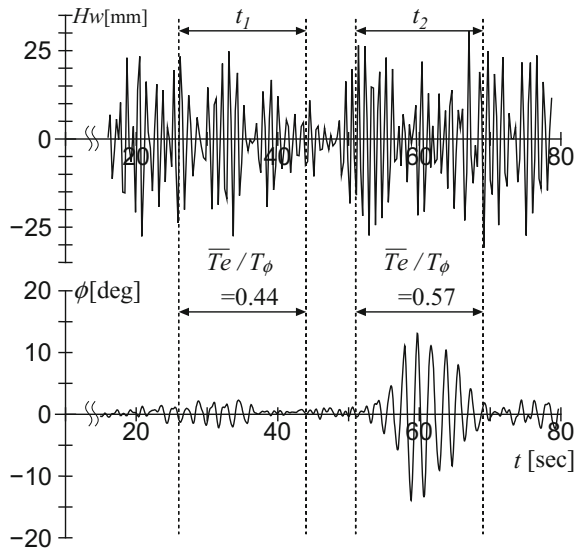


Figure 29.13 shows time histories of measured wave height and rolling at $H_w = 0.06$ m. In this figure, the ratios of mean encounter wave period to the roll natural period for small amplitude (T_e/T_ϕ) at t_1 and t_2 are also shown. The mean wave heights at t_1 and t_2 are almost same. From this figure, it is found that oscillatory rolling does not occur at t_1 ($T_e/T_\phi < 0.5$), and oscillatory rolling occurs at t_2 ($T_e/T_\phi > 0.5$).

In the Pierson-Moskowitz spectrum expressed by Eq. (29.2), increase in significant wave height causes increase in mean wave period, therefore the occurrence probability of a wave group containing frequency component of $T_e/T_\phi > 0.5$ mainly also becomes higher. On the other hand, the roll natural period becomes longer according to increase in roll amplitude. Therefore, rolling may resonate the wave group containing frequency component of $T_e/T_\phi > 0.5$ mainly.

29.5 Roll Measuring in Head Waves of Two Different Wave Period

In the roll measurement in irregular head waves, when mean wave period of group waves is $T_e/T_\phi > 0.5$, oscillatory rolling occurs. In order to investigate its reasons, the roll measurements are carried out in the waves which are generated by the superposition of two sine waves having different periods. One of two different periods is half ($T_e/T_\phi = 0.5$) of the roll natural period for small amplitude. Moreover, the wave heights of two sine waves are different. (In the following, the component with higher wave height is called Main-wave.) Experimental conditions are shown in Table 29.4 with the results.

In Table 29.4, measured roll amplitude is shown. The results show that oscillatory rolling occurs when period of Main-wave is $T_e/T_\phi = 0.50\text{--}0.61$. As the results, it is confirmed that rolling can resonate with a wave with $T_e/T_\phi = 0.50\text{--}0.61$ and it is supposed that oscillatory rolling may occur in a frame of wide line.

29.6 Numerical Simulation

By utilizing the numerical simulation model (Hashimoto and Umeda 2010), the effects of nonlinearity of *GZ*-curve on the occurrence of parametric rolling are investigated. In the simulation model, a 3DOF sway-heave-roll motion is solved in time-domain based on a nonlinear strip method in which dynamic components, i.e. radiation and diffraction forces, are calculated for an asymmetric submerged hull due to roll. Hydrodynamic forces for the heave and diffraction modes are determined

Table 29.4 Measred results

	T_e/T_ϕ ($H_w = 0.01$ m)						
T_e/T_ϕ ($H_w = 0.04$ m)	0.39	0.45	0.50	0.55	0.61	0.66	0.71
0.39			×				
0.45		×	×				
0.50	10.4	14.1		18.4	15.4	18.3	16.8
0.55			8.3				
0.61			16.0				
0.66			×			×	
0.71			×				×

ϕ [deg]: oscillatory rolling occurs

×: oscillatory rolling does not occur

Colored: oscillatory rolling occurs in regular waves

at the encounter frequency and those for the sway and roll modes are done at the half the encounter frequency.

In order to control the nonlinearity of GZ -curve, the breadth-draft ratio (B/d) of original model is changed under the constant displacement. Figures 29.14 and 29.15 show modified body plans and GZ -curves. GM for each modified model is adjusted to the same GM as the original model. Moreover, in order to make sure the characteristics of ΔGM of the original and modified models, the estimated ΔGM by the simplified method (Umeda et al. 2011) are shown in Fig. 29.16.

Figure 29.17 shows the numerical results for the original model. The calculated results show large amplitude parametric rolling occurs in the wide range over $T_e/T_\phi = 0.5$ and the numerical result shows a good agreement with the measured results.

Figures 29.18, 29.19 and 29.20 shows the calculated results for the modified models. These results show the roll amplitudes in the range over $T_e/T_\phi = 0.5$ become larger according to the increase in nonlinearity of GZ -curve.

Fig. 29.14 Body plan in real scale. ($B/d = 3.2, 3.0, 2.5$)

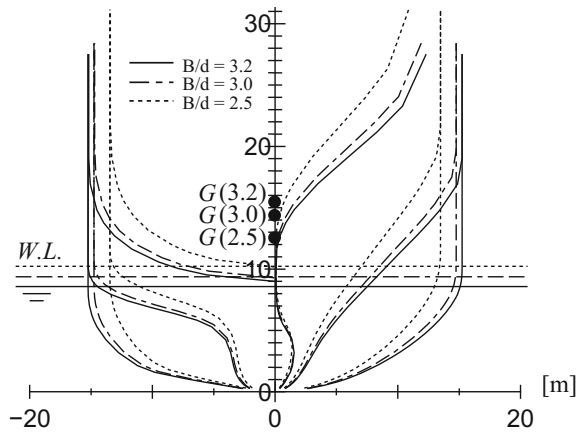


Fig. 29.15 GZ -curve of the model in real scale. ($B/d = 3.584, 3.2, 3.0, 2.5$)

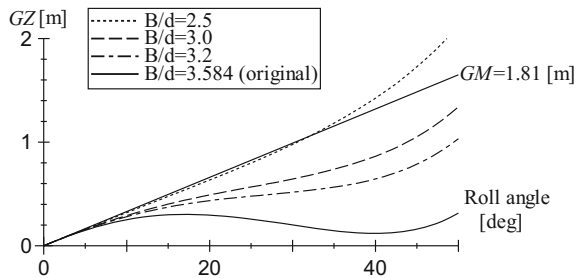


Fig. 29.16 Variation of GM caused by change of water surface of the models in real scale. ($B/d = 3.584, 3.2, 3.0, 2.5$)

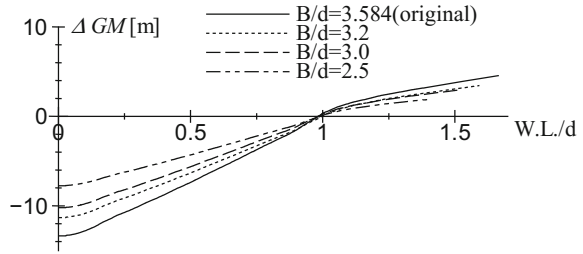


Fig. 29.17 Calculated roll amplitude in regular head waves at $Fn = 0.083$. ($B/d = 3.584$)

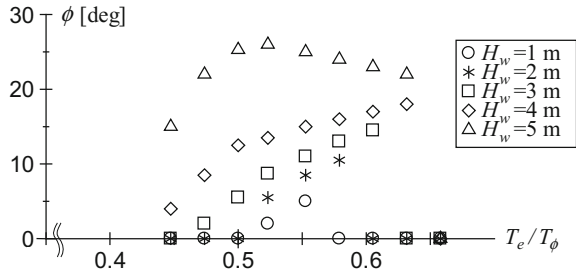


Fig. 29.18 Calculated roll amplitude in regular head waves at $Fn = 0.083$. ($B/d = 3.2$)

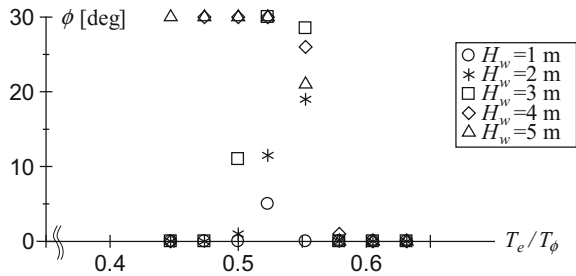
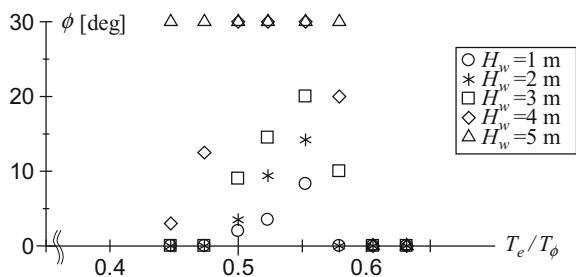


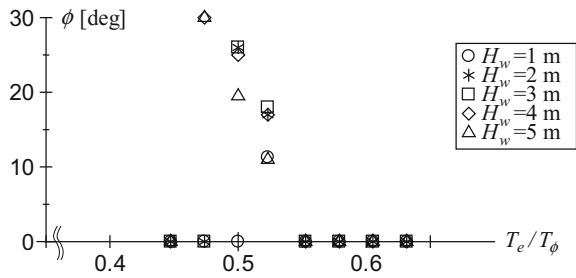
Fig. 29.19 Calculated roll amplitude in regular head waves at $Fn = 0.083$. ($B/d = 3.0$)



29.7 Conclusions

In this study, the roll characteristics of a wide breadth and shallow draft vessel in head waves are investigated. And the following conclusions are obtained.

Fig. 29.20 Calculated roll amplitude in regular head waves at $Fn = 0.083$. ($B/d = 2.5$)



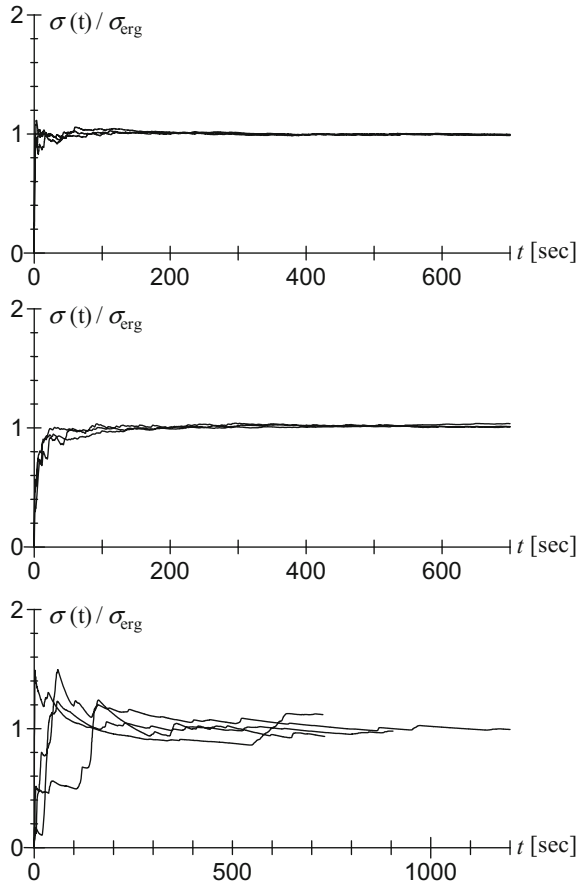
- In regular head waves, a oscillatory rolling occurs at wider range of encounter frequency than that of a conventional vessel. Especially, in the range of $T_e/T_\phi > 0.5$, a oscillatory rolling is caused by large wave height and roll amplitude becomes large.
- Numerical simulations demonstrate that the large amplitude parametric rolling occurs in the wide range over $T_e/T_\phi = 0.5$ because of the strong nonlinearity of GZ-curves.
- There is the possibility that slowdown increases roll amplitude, when parametric rolling occurs at $\lambda/L_{pp} = 1.0$.
- It is confirmed by simplified estimation that this phenomenon is caused by the following scenario. Slowdown decreases roll damping, and roll amplitude becomes large. On the other hand, roll natural period becomes longer with increase in roll amplitude. Therefore, rolling resonates with increased wave encounter period by slowdown.
- In irregular head waves with a Pierson-Moskowitz spectrum, a oscillatory rolling is caused by resonating with the group waves which contain the frequency component of $T_e/T_\phi > 0.5$ mainly.

Appendix

The Number of Times of Test in Irregular Head Waves

From wave height, pitch motion and roll motion, each variance and ensemble mean by Eqs. (29.3), (29.4). Figure 29.21 shows calculated result. In these figure, a vertical axis is a ratio ensemble mean to standard deviation. Upper and middle figure uses 20 samples and bottom figure uses 30 samples. (1 sample = 40 s) From upper and middle figure, it is found that wave height and pitch motion convergence with 5 samples. On the other hand, roll motion does not converge until 15 samples. So, this study uses 20 samples.

Fig. 29.21 Standard deviation of wave elevation, pitching and rolling. (1/3 significant wave height = 0.04, 0.05, 0.06 m)



$$\sigma^2(t) = \sum_{j=1}^{n_s} \frac{(X_j(t_j) - \bar{X}(t))^2}{n - 1} \tag{29.3}$$

$$\sigma_{erg}^2 = \frac{\sum_{i=1}^N \sum_{j=1}^n \frac{(X_i(t_j) - \bar{X}_i)^2}{n-1}}{N} \tag{29.4}$$

References

Taguchi H, Ishida S, Sawada H, Minami M (2006) Model Experiment on Parametric Rolling of a Post-Panamax Containership in Head Waves. Proceedings of the Ninth International Conference on Stability of Ships and Ocean Vehicles.

Hashimoto H, Umeda N (2010) A Study on Quantitative Prediction of Parametric Roll in Regular Waves. Proceedings of the 11th International Ship Stability Workshop: 295–301.

- Tai Y, Ohashi T, Katayama T, Ikeda Y (2011) An Experimental Study on Stability of a Shallow Draft Vessel in Beam Seas. *Journal of the Japan Society of Naval Architects and Ocean Engineers* 14: 47–54.
- Hashimoto H, Sueyoshi M, Minegaki S (2007) An Estimation of the Anti-Rolling Tank Performance for Parametric Rolling Prevention. *Journal of the Japan Society of Naval Architects and Ocean Engineers* 6: 305–311.
- Ikeda Y (2004) Prediction Methods of Roll Damping of Ships and Their Application to Determine Optimum Stabilization Devices. *Marine Technology* 41:89–93.
- Katayama T, Taniguchi T, Umeda N (2009) An Experimental Study on Parametric Rolling of a High Speed Trimaran in Head Seas. *Journal of the Japan Society of Naval Architects and Ocean Engineers* 10:57–63.
- Spyrou KJ, Tigkas I, Scanferla G, Pallikaropoulos N, Themelis N (2008) Prediction potential of the parametric rolling behaviour of a post-panamax containership, *Ocean Engineering*, 35, 11, pp. 1235–1234.
- Umeda N, Hashimoto H, Tsukamoto I, Sogawa Y (2011) Estimation of Parametric Roll in Random Seaways. In Fossen TI, Nijmeijer H (eds) *Parametric Resonance in Dynamical Systems*. Springer, 45–52